Visualising Cerebral Asymmetry

P. Marais, R. Guillemaud, M. Sakuma, A. Zisserman and M. Brady
Robotics Research Group
Department of Engineering Science
University of Oxford
Oxford OX1 3PJ

Abstract

We describe techniques for visualising and measuring the asymmetry of the cerebral hemispheres based on MRI scans. These techniques improve on previous approaches in two ways: firstly, unlike voxel based methods, measurements are not limited to voxel discretisation scales; secondly, the symmetry measurements are not slice based, but are inherently 3D. This avoids the errors in slice based measurements arising from shape distortions introduced by mis-alignment between the head and MRI machine.

We focus primarily on 'sparse' MRI data sets in which the slices are non-contiguous and widely spaced, since these constitute an important source of data in longitudinal neurological studies. Two visualisations of asymmetry are presented. The first is 3D and enables an immediate qualitative appreciation of the disposition of the asymmetry. The second is a 2D rendering of the *symmetry map*, a quantitative measure of asymmetry across the brain.

1 Introduction

The objective of this work is the visualisation and measurement of cerebral asymmetry, i.e. the disparity of the left and right hemispheres at corresponding points about the hemispheric divide. Normal people have a noticeable cerebral asymmetry; this is exhibited (usually) by the left hemisphere being of greater size at the back of the brain than the corresponding region on the right, while the opposite holds at the front of the brain. This distribution of asymmetry is often termed 'torsion'. A number of researchers [1, 4, 5, 10, 12] have suggested that the brains of schizophrenic patients experience a pronounced loss of asymmetry during the progression of the disease. The purpose of this work is to verify and quantify this effect. A large database of *sparse* MRI scans, covering a period of several years, is available for this purpose. In this context, 'sparse' means that the individual images comprising the volumetric data are non-contiguous, with large gaps between the slices.

The asymmetry effects are quite subtle in places — around voxel precision — and for this reason it is very important that accurate, undistorted, geometric measurements are made. Accurate measurements are achieved here at sub-pixel/voxel precision by using snakes to delineate the regions of interest. This is described in Section 2. The problem of geometric distortion has often been ignored in previous measurements of asymmetry. If the patient's head is mis-aligned with the principal imaging axes of the machine, then cosine foreshortening will severely distort measurements based on relative areas or lengths. This problem is avoided here by computing a symmetry plane in 3D, and referring symmetry measurements to this plane using constructions in 3D. The plane is defined as the mid-saggital (MS) plane — the inter-hemispheric region of the brain — and it is obtained by locating it's intersection within each slice. This is described in Section 3.

There are two other distortions that must be considered. First, an intensity distortion resulting from the *bias field* which originates from inhomogeneities in the RF coils. The bias field is a low frequency field which has a multiplicative effect on the scan, limiting the contrast between tissue classes and smoothly changing grey levels of the same tissue class within an image. This makes tissue classification and, consequently, segmentation, more difficult. Intensity correction against this field is described in [8, 11]. Second, a geometric distortion due to the non-linearity of the magnetic field gradient which increases as one moves towards the periphery of the bore. For this reason measurements can vary slightly depending on the patient's position in the machine. We do not currently model this distortion.

The steps in computing the symmetry visualisations are described in the following sections: The bias-corrected MRI is first segmented using the snake-based method to extract left and right hemisphere boundaries (Section 2). These curves, located to sub-pixel accuracy by the snake, are then used to construct a surface mesh for each hemisphere (Section 2). The mid-saggital curves are also extracted using snakes, and these curves define the 3D symmetry plane (Section 3). A qualitative visualisation of asymmetry is then obtained by reflecting the mesh of one hemisphere in the MS plane, and comparing it to the other hemisphere (Section 4). A quantitative 2D symmetry map is produced by plotting the signed difference of the perpendicular distances from the plane to the hemisphere surfaces over the MS plane.

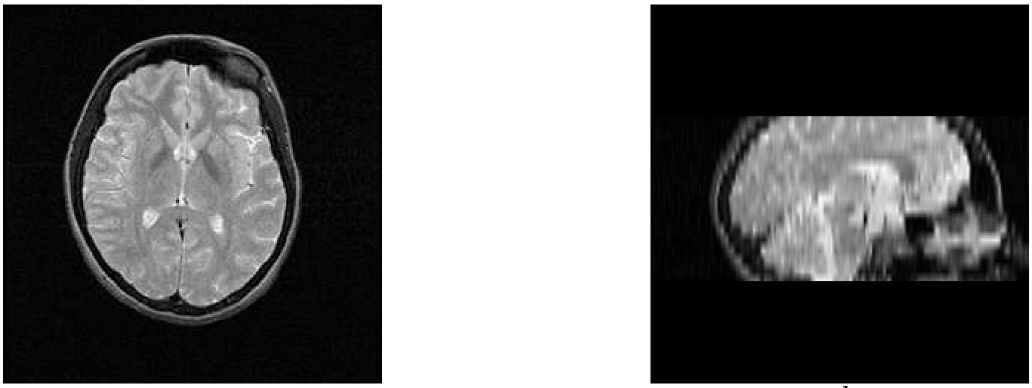

a b

Figure 1: MRI scans. (a) an individual MRI slice. (b) an orthogonal section through the entire sparse MRI data set. The affects of poor sampling in the acquisition direction are clearly visible. The images are of size 256x256 and the scan comprised 21 such scans at a voxel size of 0.9x0.9x5.0mm^3 with gaps of 2mm between slices, giving an effective voxel size of 0.9x0.9x7.0mm^3.

2 Segmentation with Enhanced B-spline Snakes

MRI data is acquired as a sequence of (possibly non-contiguous) slices through an object. The slice thickness varies from under one millimetre to about 5mm, while the slice gap, if present may be as large as 2mm. As a precursor to the analysis and visualisation step, we have to segment the objects of interest (in this case the left and right cerebrum) from the other structures present in the data set.

We use approximating B-spline *snakes* [2] to delineate the boundaries of the relevant structures. Snakes are dynamic contours which are attracted to image features, such as edges.

The B-spline snakes we employ are different from the 'standard' snake approach [9] — rather than using a wide potential function to guide the edge search, these snakes utilise 1D Canny [3] edge detectors to search for gradient discontinuities in a direction perpendicular to the snake boundary at

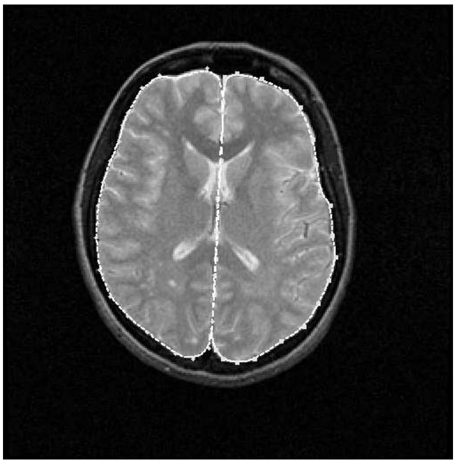

Figure 2: Segmentation. The snakes which constitute the boundary of the left and right hemispheres are shown. They have been thickened to enable easier viewing.

evenly spaced points along the snake's length. In contrast to voxel/pixel based methods, such snakes are able to isolate contours to sub-pixel accuracy using standard methods of sub-pixel edge detection. The 1D edge detection is restricted to a *search scale*, which limits the distance at which the snake will sense edges. This is important in cluttered data sets, where there are many potential edge associations within slices. Since the problem of finding the edges is essentially reduced to a one-dimensional one, the computational cost associated with these snakes is low.

Different biological structures have different edge characteristics, and the edge search is tuned to these characteristics. For example, a valley detector is used to isolate the mid-saggital line, while a contrast sensitive step detector is used to isolate the external cerebral boundary. Furthermore, the features for which the snake searches are allowed to vary along the curve, permitting *a priori* information about boundary structure to be incorporated into the segmentation process. The bias correction helps ensure that step contrast is fairly constant along the boundary.

After the edge search has been completed, the snake is fitted as closely as possible to the resulting edge data (by spline regression). When the snake has 'locked on' to a boundary in one layer, it proceeds to 'track' the boundary through succeeding slices. A linear prediction scheme is used for the tracking, so that the the snake is initialised as close as possible to it's successor (on the next slice) curve by extrapolating from past curve motion.

The end result of the segmentation step is a series of closed curves representing the boundary of the cerebral hemisphere in each cross sectional scan, see Figure 3. These curves are then linked to form a quadrilateral surface mesh, by joining a number of points along the curve length to corresponding points on neighbouring curves, see Figure 4. In more detail, a transverse plane is intersected with the curves, and the common intersection point serves as an initial point for the re-sampling of the curve data (the curves may be resampled precisely through the B-spline equations). This method works well provided that the object has cylindrical topology and that the intersecting plane can be chosen to intersect all the curves. In general this has proved satisfactory.

3 Extracting the Mid-Saggital Plane

To obtain points on the MS plane, a snake is initialised along a mid-saggital line in one slice, and allowed to propagate through the other slices under supervision. Once the snake has propagated through a number of slices, the process is terminated and the mid-saggital line data (control points

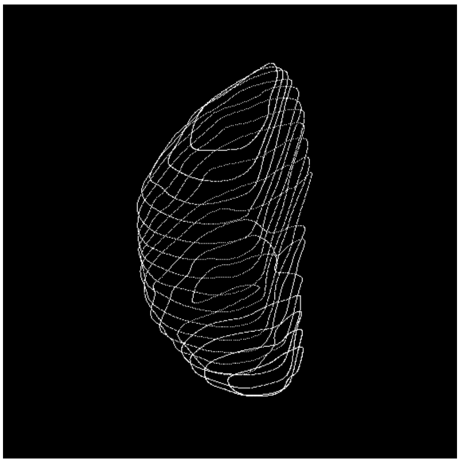

Figure 3: Contour description. The snakes which constitute the boundary of the left hemisphere are shown. Note the wide spacing of the sampled contours arising from the sparse MR scans.

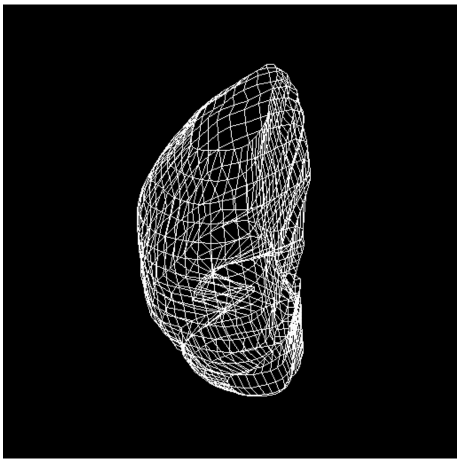

a

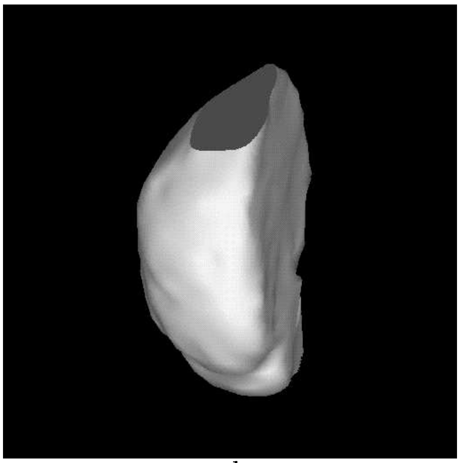

b

Figure 4: Surface rendering. The contour description provided by the snake segmentation is resampled and a mesh generated (a). This is used in subsequent visualisation and symmetry computations. A shaded mesh is shown in (b).

representing the curve) from these slices are used as the 3D data set for an *orthogonal regression* plane fit. This yields the plane in 3D which minimizes the sum of squared perpendicular distances from the points in the data set to the plane [7].

The plane-fitting method was evaluated over 25 scans. The standard deviation of the sample points from the plane was between 1 and 1.5 mm (the size of a voxel), while the maximum error of the fit was 4mm, see Figure 6. In other words, the plane constitutes a reasonable approximation to the inter-hemispheric fissure for the study of asymmetry.

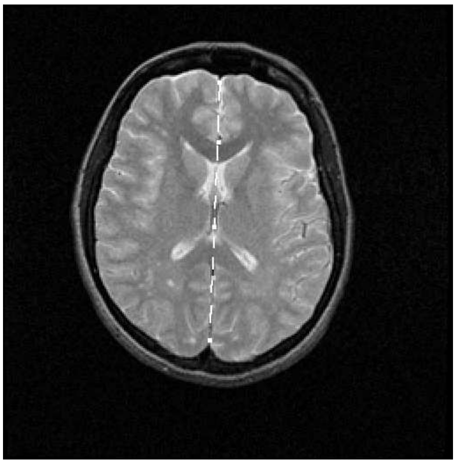

Figure 5: Mid-Saggital snake. One of the snakes used to follow the mid-saggital line. A set of such snakes is used to generate an approximation to the mid-saggital plane.

The idea of using an inter-hemispheric plane to correct for the orientation of the brain in the MRI is not a new one. Some attempts have already been made to estimate this plane, as in the ANALYSE software. This generally involves the manual selection of a limited number of landmarks within the brain to define the location of the plane. The definition of the MS plane provides a consistently oriented coordinate frame.

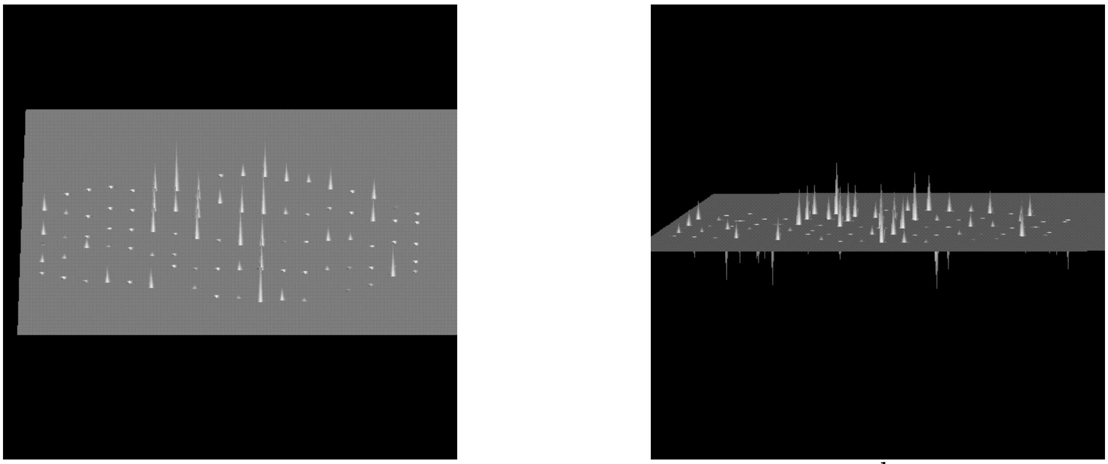

a

b

Figure 6: These two figures show the error associated with the orthogonal regression plane fit. The peaks are the perpendicular discrepancy between the plane and the individual MS sample points. The max peak size is 2.2mm. Two views are presented to illustrate the fact that the error is well distributed on both sides of the plane.

In our application, however, we are not simply interested in the MS plane as a means of orienting our data set, but also as the basis for cerebral symmetry measurements. In this case the accuracy of the plane must be much higher, since the plane is used to define the reference/basic geometric information for the asymmetry computation.

4 Visualising the symmetry disparity

A direct visualisation of asymmetry is achieved by reflecting the left or right hemisphere through the symmetry plane onto it's partner. This is illustrated in figure 7. The dark surface is the reflected mesh, Gouraud shaded for the visualisation.

While the reflected surface visualisation is useful for qualitative understanding, there is a need to generate a more quantitative description of the asymmetry. One means of doing this is to produce a *symmetry map* — i.e. a surface representing asymmetry over the MS plane. The asymmetry measure used is the signed difference in distances from the MS plane to the left and right cerebral surfaces in a direction perpendicular to the plane. Examples are shown in Figures 8 and 9.

5 Conclusion

The visualisation of cerebral asymmetries has tremendous potential as a diagnostic aid for neurological diseases which alter the morphology of the brain, such as schizophrenia. Because the approach we have developed is adapted to deal with the presence of the bias field as well as providing insulation against machine-patient misalignment, we are able to achieve a robust segmentation, and accurate measurements and visualisation of asymmetry. In particular, the techniques are usable for sparse MRI data sets (which have proved very difficult to analyse using existing techniques). The generation of appropriate visualisation ensures that the results are displayed in a manner which is easy to assimilate: the reflection provides an indication of the relative sizes of corresponding cerebral regions, while the symmetry map enables measurements of the distribution of the asymmetry.

5.1 Future Work

There are several areas of this work which we are currently refining:

Improving the robustness of the segmentation The segmentation method we employ already uses *a priori* knowledge to guide its progress. However, we would like to build in model constraints e.g. the notion of expected geometric structure, while providing for deviations from this model causes by inter-patient variability and/or pathology. We are examining the possibility of employing a skeletal representation to embody the geometric constraints. There is also a need to improve the mesh generation, since there are certain cases which are currently problematic.

Developing more useful symmetry measures The usual L-R symmetry measure, $\frac{M(L)-M(R)}{M(L)+M(R)}$, where $M(.)$ represents some measure applied to the L or R hemisphere, is not able to discriminate really useful asymmetry features. While the symmetry map we employ provides a dense estimate of local asymmetry across the MS plane, it seems that for a really useful analysis one requires some deeper measure of brain dissimilarity than the LR metric. It may be that a surface matching technique such as that developed by Feldmar [6], which attempts to find the best (locally) affine fit between the two surfaces, provides the necessary generalization. One could define a *surface map* on the reference surface which provides data on the normal separation between the two surfaces at any given point.

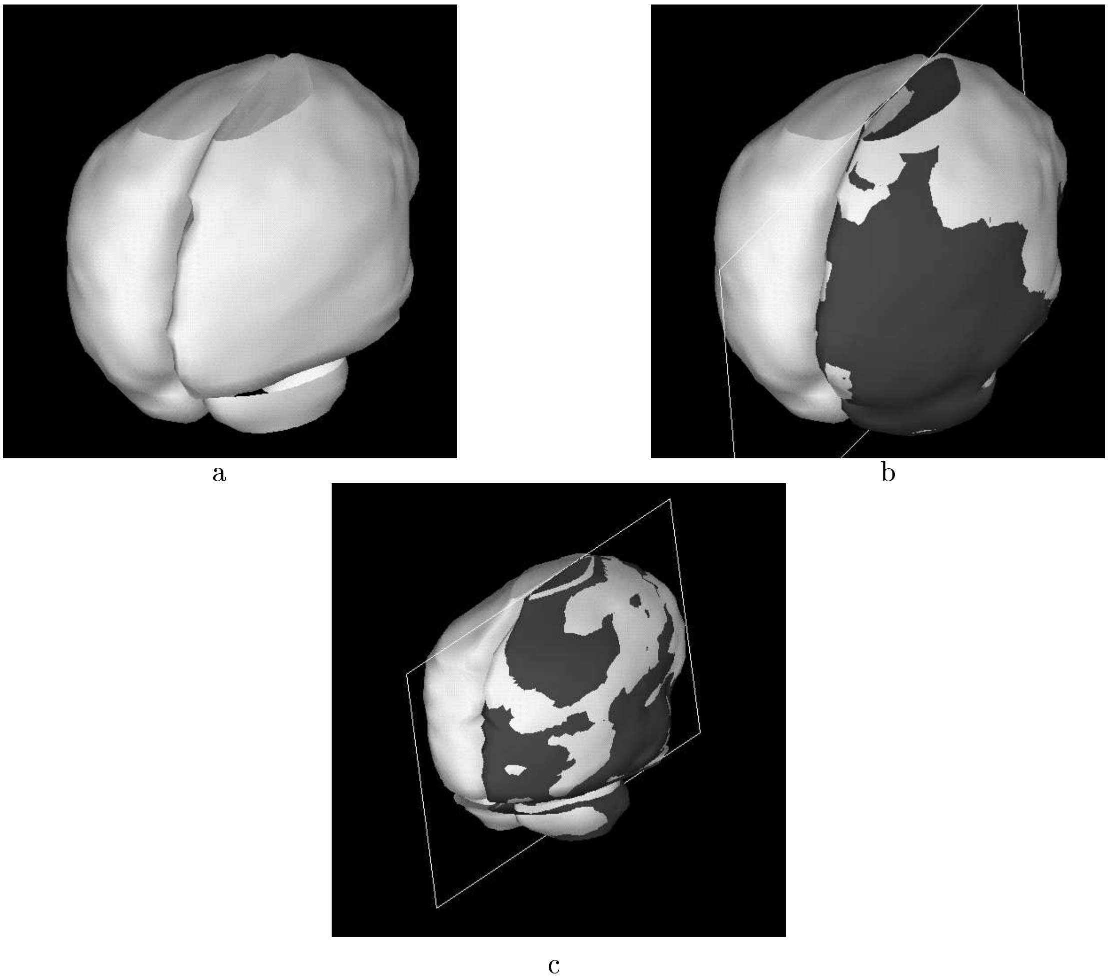

Figure 7: Visualising asymmetry. (a) the surface meshes representing the left and the right hemisphere obtained via the segmentation technique discussed in Section 2. (b) the left hemisphere is reflected through the MS plane (represented by the rectangle) and superimposed on the right hemisphere. This allows a qualitative appreciation of the L-R asymmetry. For example, the dark surface, which is the reflection of the left hemisphere, is visible in the right posterior region, showing that the left hemisphere is larger than the right in this region. (c) provides another example of symmetry reflection, applied to a different brain.

Figure 8: The symmetry map corresponding to Figure 7b. Dark values correspond to negative asymmetry (the right hemisphere is smaller than the left) whilst lighter values represent positive asymmetry (the right hemisphere is larger than the left). The background has been set to match the darkest value (i.e. the highest negative asymmetry). The map shows that the left hemisphere is larger than the right just above the cerebellum; this asymmetry progressively diminishes as one moves away from this region. The values of brain asymmetry are plotted here for a range of -25mm up to 25mm to allow for border effects (where the hemispheres are laterally shifted, and so misaligned). The key gives the scale of asymmetry to grey-level.

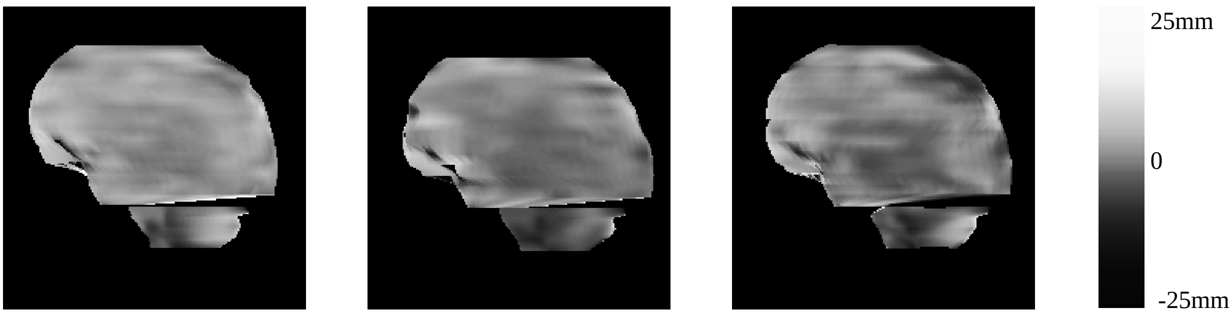

Figure 9: Evolving symmetry maps. The sequence of symmetry maps shown here are for the same patient at one year intervals. There are small but measurable changes in the asymmetry.

Acknowledgements

We would like to acknowledge the support of SUNY (Dr. L. De Lisi, Stonybrook), as well as Dr. T. Crow of the Dept. Clinical Neurology, University of Oxford. Special thanks also go to Dr. B. McDonald (Cl. Neurol., Oxford) for his assistance in preparing the data for analysis. This work was primarily supported by MRC grant G9220033.

References

[1] R. M. Bilder. Absence of regional hemispheric volume asymmetries in first-episode schizophrenia. *American Journal of Psychiatry*, 151(10):1437–1447, Oct 1994.

[2] A. Blake, R. Curwen, and A. Zisserman. A framework for spatiotemporal control in the tracking of visual contours. *Intl. Journal of Comp. Vis.*, 11(2):127–145, 1993.

[3] J.F. Canny. A computational approach to edge detection. *IEEE Transactions on Pattern Analysis and Machine Intelligence*, 8(6):679–698, 1986.

[4] T. J. Crow. Temporal lobe asymmetry as the key to the aetiology of schizophrenia. *Schizophrenia Bulletin*, 16:433—443, 1990.

[5] L. DeLisi. Loss of normal cerebral asymmetries in first-episode schizophrenia. *To appear: Archives General Psychiatry*, December 1994.

[6] J. Feldmar. *Rigid, non-rigid and projective registration of medical images.* PhD thesis, Ecole Polytechnique, 1995.

[7] G. Golub and C. Van Loan. *Matrix Computations.* John Hopkins University Press, 1983.

[8] R. Guillemaud and M. Brady. Enhancing MRI images. Submitted to VBC'96, 1996.

[9] M. Kass, A. Witkin, and Terzopoulus. Snakes: Active contour models. *Proc. First Intl. Conf. on Comput. Vis.*, pages 259–268, 1987.

[10] H. Steinmetz. Total surface of temporoparietal intrasylvian cortex: diverging left-right asymmetries. *Brain and language*, 39:357–372, 1990.

[11] W. Wells, W. Grimson, R. Kikinis, and F. Jolesz. In-vivo intensity correction and segmentation of magnetic resonance image data. *AAAI Med. Imaging*, pages 199–202, April 1994.

[12] R. Zipursky. Widespread cerebral gray matter volume deficits in schizophrenia. *Archives General Psychiatry*, 49:195–205, March 1992.